Cloud and Water Vapor Feedbacks in a Vertical Energy-Balance Model with Maximum Entropy Production

BIAO WANG

State Key Laboratory of Numerical Modeling for Atmospheric Sciences and Geophysical Fluid Dynamics, Institute of Atmospheric Physics, Chinese Academy of Science, Beijing, China

TERUYUKI NAKAJIMA

Center for Climate System Research, Tokyo University, Tokyo, Japan

GUANGYU SHI

State Key Laboratory of Numerical Modeling for Atmospheric Sciences and Geophysical Fluid Dynamics, Institute of Atmospheric Physics, Chinese Academy of Science, Beijing, China

(Manuscript received 28 November 2007, in final form 20 May 2008)

ABSTRACT

A vertically one-dimensional model is developed with cloud fraction constrained by the maximum entropy production (MEP) principle. The model reasonably reproduces the global mean climate with its surface temperature, radiation and heat fluxes, cloud fraction, and lapse rate. The maximum convection hypothesis in Paltridge's models is related to the MEP principle, and the MEP state of climate is approximately equivalent to that with the maximum lapse rate. The sensitivity investigation about the model assumptions and the prescribed parameters show that the model is considerably robust in simulating the global mean climate. With the MEP constraint, the feedbacks of cloud and water vapor to external forcings, such as changes of CO_2 concentration, solar incidence, and surface albedo, are evaluated. While water vapor always behaves as a strong positive feedback, cloud feedbacks to the different forcings are different, in both magnitude and sign. The modeled feedback of cloud fraction to the forcing resulting from surface albedo variation seems in good agreement with the observed seasonal variation of the global cloud fraction.

1. Introduction

Climate change can be considered the response of the climate system to external forcings, such as radiative forcing resulting from greenhouse gases (GHGs), atmospheric aerosols, etc. While the understanding of the external forcings remains with uncertainties, the response of the system is largely complicated by a variety of feedback processes, especially those involving clouds and water vapor (CWV) in the atmosphere. Water vapor is an important greenhouse gas and clouds have a GHGs-like effect on outgoing longwave radiation. In addition, clouds reflect incoming shortwave radiation, which reduces energy input to the system. Furthermore, the cloud effects are determined by various microscopic and macroscopic properties of clouds, which, along with water vapor, respond quickly to changes of the system in complicated spatial patterns. Water vapor is transported by turbulent and circulation processes, while clouds and water vapor transform into each other, associated with the exchange of latent heat that in return influences atmospheric circulations. The climatic feedbacks of CWV have long been regarded as one of the most important sources of uncertainty in the prediction of climate change (Houghton et al. 2001).

As with the complicated processes involved in the CWV feedbacks, some overall thermodynamic principles may be useful in providing a macroscopic constraint on the net effect of the interactions. With a simple energy balance model, Paltridge (1975, 1978) showed that the overall entropy production (EP) rate of turbulent processes of the climate system tends to take its maximum value when the modeled circulation intensity and the distribution of temperature and cloudiness are close to those observed in the climate

Corresponding author address: Biao Wang, Institute of Atmospheric Physics, Chinese Academy of Science, Beijing 100029, China.
E-mail: wangbiao@post.iap.ac.cn

DOI: 10.1175/2008JCLI2349.1

system. An updated version of the model has been used to investigate the feedbacks of cloud, water vapor, and lapse rate to the doubled CO_2 in the atmosphere (Paltridge et al. 2007). The result indicates that clouds in a long-term average, no matter how complicated the microphysics and dynamics involved, have to be under the constraint of the general thermodynamic condition. Paltridge's work has inspired a number of succeeding studies that either explore the underlying mechanisms or find further evidence and application in climate studies (e.g., Grassl 1981; Kleidon et al. 2003; Mobbs 1982; Nicolis and Nicolis 1980; O'Brien and Stephens 1995; Ozawa and Ohmura 1997; Ozawa et al. 2001; Paltridge 2001; Pujol 2003; Pujol and Llebot 1999a,b, 2000a,b; Pujol and Fort 2002; Shutts 1981; Sohn and Smith 1993, 1994). The so-called maximum entropy production (MEP) hypothesis has been suggested to be a macroscopic principle that is applicable to nonlinear systems with many degrees of freedom for dynamic motion, as the climate system seems to be (Dewar 2003; Kleidon and Lorenz 2005; Lorenz 2003; Ozawa et al. 2003). Although the MEP hypothesis's applicability as a general principle to the climate system has not been fully justified, it may work well for the problem with appropriate constraints (Goody 2007).

In addition to the MEP principle, Paltridge's original models included another hypothesis of maximum convective heat transport, which was suggested as being compatible with the broad principle of maximum dissipation and MEP (Paltridge 1978). However, the convection hypothesis could not be shown to be identical to the MEP principle, because the entropy production resulting from the vertical heat transport also depends on the vertical temperature gradient (or lapse rate) of the atmosphere, which was not resolved in Paltridge's models. O'Brien and Stephens (1995) highlighted the role of the convection hypothesis as being as important for the model as the MEP principle to obtaining the realistic climate. With more and more modeling evidence supporting the MEP principle, the vertical thermal structure of the atmosphere associated with the convection hypothesis has to be resolved to apply the MEP principle as a general constraint to the climate system. So far, a handful of studies have discussed the entropy production in the vertical dimension. Ozawa and Ohmura (1997) investigated the vertical dimension with a column model of gray atmosphere and suggested that the MEP principle may be potentially applied to the convective process to obtain the observed vertical thermal structure of the atmosphere. Pujol and Fort (2002) and Pujol (2003) reexamined the applicability of the MEP constraint on the lapse rate indirectly in one-dimensional radiative-convective models, with the MEP constraint on the temperature difference between ground and near-ground air and the eddy heat diffusivity, respectively. These vertical 1D models simply treated irradiance in gray or semigray atmospheres without explicit treatment of cloud. On the other hand, the MEP climate has been shown to be rather sensitive to the treatment of water vapor concentration in a rather complicated zonal mean 2D model (Noda and Tokioka 1983). To study the MEP constraint on the vertical turbulent processes, explicit accounts of cloud and water vapor effects on radiative transfer is required, associated with the detailed representation of radiative properties of the atmosphere with its nongray characters.

In the following sections, a vertical one-dimensional energy balance model is introduced. The model employs a complete radiation scheme to explicitly evaluate the radiation effects of CWV, as well as other trace species in the atmosphere. The MEP criterion is used to determine the fraction of clouds and water vapor concentration. Numerical experiments show the model responses to the climate forcings resulting from the different agents and the potential capability of the MEP principle to account for the climate feedbacks of clouds, water vapor, and the associated lapse-rate change. Section 2 describes model assumptions and the algorithm; section 3 presents the results of the model in simulating the current state of the atmosphere and its sensitivity to the assumptions and model parameters; section 4 investigates the cloud water vapor feedbacks of the model to some external forcings; and section 5 further discusses the results and their implications.

2. Model description

The model used in this study is a vertically one-dimensional energy balance model. Because there is no lateral boundary exchange considered in this work, the model is supposed to represent the global mean state of the atmosphere, assuming that the system is in energy balance. At the top of the atmosphere, the incoming shortwave radiation is balanced with the outgoing longwave radiation; at the bottom, the net radiation is balanced with the vertical sensible and latent heat fluxes. In addition, the irradiance divergence within the atmospheric column should be balanced with the convergence of the energy fluxes associated with the convection,

$$\nabla \cdot R - \nabla \cdot F = 0, \tag{1}$$

where R is the downward net irradiance and F is the upward convective flux density (i.e., for per unit area). With the boundary condition that there is not net energy exchange at the top of the atmosphere (TOA) or

the surface, the energy balance equation is simply written as

$$R - F = 0, \tag{2}$$

which should be satisfied at each level of the atmosphere.

The other equations and assumptions used in the model are described in the following subsections.

a. Radiation scheme

A comprehensive radiation scheme is used in the model to explicitly evaluate the radiative effects of clouds and water vapor, as well as other species like CO_2, CH_4, O_3, O_2, N_2O, and aerosols, etc. The scheme is based on a *k*-distribution representation of gas absorption with 23 and 21 spectral intervals, respectively, for shortwave and longwave radiation. The δ-Eddington two-stream formulation and the two-stream source function technique developed by Toon et al. (1989) are used to calculate shortwave and longwave irradiance, respectively. The radiative properties of gases, clouds, and aerosols are parameterized in terms of optical depth, single scattering albedo, and asymmetrical factor. The dependence of radiative properties of water clouds on effective radius are parameterized after Hu and Stamnes (1993). A simplified version of the radiation scheme with fewer spectral intervals has been used in GCMs developed by the State Key Laboratory of Numerical Modeling for Atmospheric Sciences and Geophysical Fluid Dynamics, Institute of Atmospheric Physics, Chinese Academy of Science (LASG/IAP/CAS; Wang et al. 2000).

b. Convective energy flux

The convection is formally driven by the vertical temperature gradient or lapse rate in the model. To account for the feedback involving lapse-rate change, the lapse rate in the model is taken as variable rather than prescribed, as in some of convective adjustment schemes. As suggested by Ozawa and Ohmura (1997), the vertical thermal structure of the atmosphere is likely constrained with the MEP principle; however, to focus on the role of CWV, the convective energy flux is simply assumed to be linearly proportional to the lapse rate γ ($\gamma = -dT/dz$, where T and z are the temperature and altitude, respectively), given that the lapse rate exceeds a critical value γ_c,

$$F = \begin{cases} k_c p(\gamma - \gamma_c), & \text{when} \quad \gamma > \gamma_c \\ 0, & \text{when} \quad \gamma \le \gamma_c \end{cases}, \tag{3}$$

where p is the pressure and k_c is a proportional coefficient. This relation is similar to that used by Pujol (2003) following the mixing length theory, but as an approximation, the latent heat component is implicitly included in the general flux without explicit dependence on the specific humidity. In principle, the k_c–γ_c relation can be determined empirically with the relationship between global mean convective flux and lapse rate, that is,

$$k_c = \frac{F_{\text{obs}}}{p_{\text{obs}}(6.5 - \gamma_c)}, \tag{4}$$

where 6.5 K km^{-1} is taken as the global mean lapse rate and the observed surface pressure $p_{\text{obs}} = 1013$ hPa. As illustrated by Kiehl and Trenberth (1997), the global mean surface convective heat flux $F_{\text{obs}} = 102$ W m^{-2}, contributed by sensible and latent heat fluxes. Here, $k_c = 15.5$ W m^{-1} K^{-1} hPa^{-1}, for example, when the effect of γ_c is ignored.

c. Cloud fraction and relative humidity

Most of the conceptual models have assumed a constant relative humidity so that the radiative path of water vapor is determined solely by atmospheric temperature. Nevertheless, a more physically based manner is to link the relative humidity to cloud fraction (e.g., Jentsch 1987; Mitchell and Ingram 1992). Walcek (1994) reviewed the correlations between cloud cover and relative humidity and found that values of the correlation coefficients increase with the horizontal averaging areas and that there is no clear "critical relative humidity" below which cloud coverage is always zero. He concluded that cloud coverage (f) decreases exponentially with relative humidity (RH), and that the cloud fraction would not be zero even if the relative humidity vanished.

This work is dedicated to the global scale, and for convenience a linear relationship between cloud fraction and relative humidity is assumed for the model levels below the cloud-top altitude,

$$\text{RH} = C_1 f + C_2. \tag{5}$$

The coefficients C_1 and C_2 can be inferred from the datasets like International Satellite Cloud Climatology Project (ISCCP) D2 (Rossow and Schiffer 1999), which includes data about precipitable water (w), cloud fraction, and temperature (T). A proxy of the relative humidity is defined as

$$\text{RH}^* = w/Q_{\text{sat}}, \tag{6}$$

where Q_{sat} is the saturated partial pressure, which is a function of temperature. It is easy to see that

$$C_1 \frac{f}{\mathrm{RH}} = \frac{d\mathrm{RH}/\mathrm{RH}}{df/f} \approx \frac{d\mathrm{RH}^*/\mathrm{RH}^*}{df/f}. \quad (7)$$

The value of the right-hand side of the equation can be obtained from best fitting the normalized deviation of RH* and f, and equals 1.97 for the ISCCP D2 datasets of cloud climatology for 1989–93.

The model then takes $C_1 = 2.24$, with the current global annual mean values of RH and f, which are taken as 77% (Manabe and Wetherald 1967) and 67.6% (Rossow and Schiffer 1999), respectively. The C_2 then is -0.744, determined by

$$C_2 = \overline{\mathrm{RH}} - C_1 \bar{f}. \quad (8)$$

It should be noted that the equation is supposed to represent the general relationship between the water vapor and cloud fraction in the global scale, in contrast with the cloud parameterization schemes involved subgrid processes, and the applicability of the equation is limited to the domain closely around the mean value point($\overline{\mathrm{RH}}$, $\bar{f}$) resulting from the linearity assumption. Here, C_2 is negative and consistent with Walcek's (1994) conclusion; however, C_1 does not correspond to the first derivative of his formulation, which seems valid only at the smaller scales (<800 km). The water vapor profile above the top-of-cloud level in the model simply follows the model atmospheres (McClatchey et al. 1972). In practice, the middle-latitude winter (MLW) profile has been adopted for the RH profile above the top-of-cloud level. The choice is a little arbitrary without a priori knowledge, and another option [such as the middle-latitude summer (MLS) profile] has been tested with no qualitative difference found in the results.

d. Entropy production

The EP rate is calculated according to the thermodynamic definition of the entropy,

$$\dot{S} = \int F d\frac{1}{T}, \quad (9)$$

and the integral is practically taken from the surface to the tropopause where the upward turbulent energy flux ceases to zero. From Eq. (2), the equation is equivalent to $\dot{S} = -\int R d\ 1/T$.

To close the set of Eqs. (2), (3), and (5)–(7), the MEP criterion is used, that is, the cloud fraction has to take a value of f_{MEP} so that the resulting EP tends to the maximum, among any of the possible cloud fraction values (from 0 to 1), that is,

$$\dot{S}(f_{\mathrm{MEP}}) = \max_{0 \le f \le 1} \dot{S}(f). \quad (10)$$

e. Numerical procedure

The present version of the model takes 10 layers of the atmosphere with roughly equal geometric thickness (i.e., equal increment of logarithmic pressure), and a nearby level is set to the prescribed pressure of the cloud top (580 hPa, see section 3). The cloud is set to fill the layers between the top-of-cloud level and the surface. An iteration procedure is used to obtain the thermodynamic equilibrium state of the model. The procedure is as follow:

1) Start with an initial state (a model atmosphere) with a fixed prescribed cloud fraction; and then
2) calculate the irradiance at each level of the model with the RH defined by Eq. (5) and by the model atmosphere within the cloud layers and the other layers, respectively; and
3) obtain the required convective fluxes with Eq. (2). On the other hand, another set of the convective flux values can be calculated with Eq. (3);
4) the temperatures for each layer of the model then are adjusted with a simplex algorithm to minimize the absolute difference of the two sets of convective fluxes so that steps 2 and 3 above are repeated with the simplex procedure to obtain the equilibrium state.

The convergence criterion is

$$\left[\sum_{l=1}^{L} (\Delta F_l)^2/L\right]^{1/2} < 0.01\ \mathrm{W m^{-2}}. \quad (11)$$

Finally, the above iteration procedure is repeated for different cloud fractions (from 0 to 1); the MEP state of the model is determined to be the equilibrium solution with the maximum EP value [Eq. (10)]. For the control run to be illustrated in section 3, the maximum value of ΔF among the layers when the convergence criterion has been reached is 0.058 W m^{-2}.

It is worthwhile to note that the numerical procedure implies some mechanisms that are not represented by previous works. The changes of temperature at each step of the iteration feed back on the longwave radiation not only via Stefan–Boltzmann's law or a modified water vapor amount, but also by modifying atmospheric absorption (i.e., affecting the intensity and shape of the spectral lines of radiative gases). With Eq. (3), the structure of the troposphere in the model naturally emerges during the procedure, reaching the energy balance without a prescribed tropopause level. However, the tropopause level has not been clearly resolved (See Fig. 1b, next section) in the model results because of the still-coarse vertical resolution.

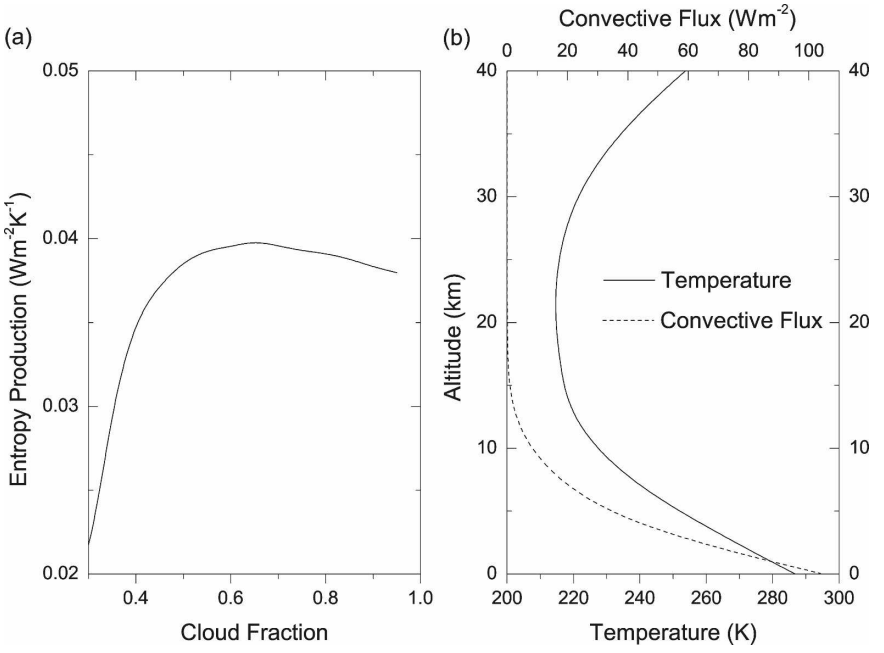

FIG. 1. (a) Modeled EP vs cloud fraction, with other input same as in the Table 1. (b) Model results of temperature and convective flux profiles for the global mean condition listed in the Table 1.

3. Model results and their sensitivities to the assumptions and parameters

Table 1 lists the results of the model for a set of control inputs. The properties of clouds (LWP, cloud-top pressure, and cloud effective radius) are after the global mean values of the ISCCP D2 dataset. The 60° of the solar zenith angle is the commonly adopted geometry for vertically one-dimensional models to represent the global mean incidence of the solar beam. The surface reflectance (0.128) is the global mean value weighted by the relative exposure area and duration to the sunlight of the global surface areas, and is therefore expected to be less than the arithmetically averaged value resulting from less weight for a higher latitude.

Given the simplicity of the model, the resulting cloud fraction, surface temperature, surface flux, and lapse rate seem reasonably close to the currently observed global mean numbers. The surface flux here refers to either the net downward radiative flux or equivalently the upward convective flux. Because the convective flux is assumed to be proportional to the temperature gradient [Eq. (3)], and the EP is approximately proportional to the products of the flux and temperature difference, the results obtained with the MEP criterion is approximately equivalent to those with the maximum lapse rate and the maximum surface flux. In other words, the cloud fraction 0.67 can be regarded as the optimum for the maximum global mean lapse rate; if the cloud fraction deviates from the value (becoming either less or more), then the lapse rate and the EP will decrease. The EP variation with the cloud fraction and the MEP results for temperature and flux profiles are illustrated in Fig. 1.

To examine the robustness of the model, sets of results are calculated with the varied coefficients in Eqs. (3) and (5). As mentioned above, k_c is determined by the observed global mean quantities (surface flux and surface pressure) and the somewhat arbitrary parameter γ_c. The model shows that, when γ_c increases from 0.0 to 4.0, associated with k_c varying according to Eq. (4), the resulting cloud fraction varies slightly within a narrow range from 0.67 to 0.62 and the EP decreases too. In other words, even if γ_c is left as a free variable, the MEP criterion will give the same result because γ_c will be constrained to be zero. However, the resulting

TABLE 1. Inputs and output results of the model for a control run representing the global and annual mean state of the climate system.

Control inputs	Results
Solar zenith angle: 60°	Cloud fraction: 0.67
Surface reflectance: 0.128	Entropy production: 0.0398 W m^{-2} K^{-1}
Cloud water (LWP): 65.8 g m^{-2}	Surface temperature: 287 K
Cloud top pressure: 580 hPa	Surface flux: 104 W m^{-2}
Cloud effective radius: 11 μm	Lapse rate: 6.8 K km^{-1}

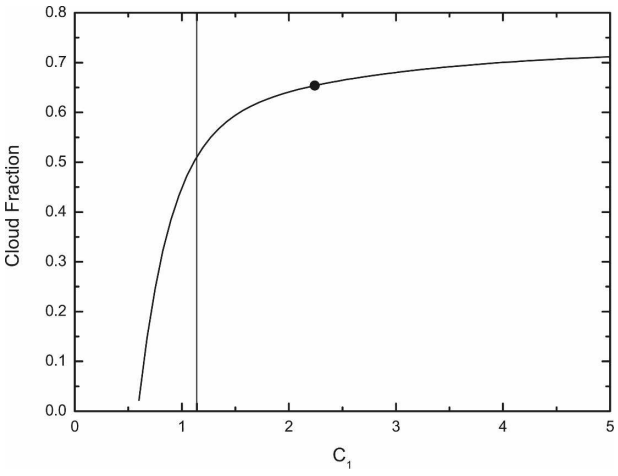

FIG. 2. The sensitivity of the modeled cloud fraction to the assumed relation between cloud fraction and RH; C_1 is defined in Eq. (5). The vertical line indicates the C_1 value when $C_2 = 0$; the single dot indicates the values adopted for the global mean condition in the model.

cloud fraction for MEP will change significantly when k_c deviates from the value deduced from Eq. (4). The result implies that k_c may not be constrained by the MEP principle to get a realistic modeling result, in contrast to that suggested by Ozawa and Ohmura (1997).

Here, C_1 represents the linear ratio between the relative humidity and cloud fraction variabilities, while C_2 is determined by C_1 and the reference relative humidity and cloud fraction [see Eq. (8)]. Given that the relative humidity is sensitive enough to the cloud fraction variation, the resulting cloud fraction is within a relatively acceptable range (Fig. 2). Also shown in the figure with a vertical line is a naturally critical point $C_1 = 1.14$ obtained for C_2 to be zero; when C_1 is above this value, the resulting variation of cloud fraction is relatively slow and within an acceptable range (0.5–0.7).

4. CWV feedbacks to external forcings

Numerical experiments are designed to investigate responses of the model to the climate forcings: CO_2 concentration, solar constant, surface albedo, cloud LWP, and cloud-droplet radius. Table 2 lists the responses of the model parameters and the sensitivities of the feedbacks by CWV to the initial forcings. To facilitate the comparison among the different forcing agents, all data in the table are normalized with the instant forcings that are evaluated with the changed forcing agents and with other parameters fixed as in the control case. The sensitivity is here defined as the ratio of the feedback of cloud and/or water vapor to the initial instant forcing. In other words, a value in the table means a change of the respective item (surface temperature, lapse rate, cloud fraction, or feedbacks) resulting from a unit forcing (i.e., 1 W m^{-2}). It has to be noted that the effects of the lapse-rate change, partly associated with change of the tropopause level not fully resolved by the model, have not been evaluated independently so that the lapse-rate feedback is indeed included in the results about the longwave feedbacks of CWV.

For each case, the water vapor feedback is positive no matter how the cloud fraction changes because the increase of water vapor amount resulting from the warming effect overwhelms that resulting from the relative humidity change in accordance with the cloud fraction. For the CO_2, solar constant and the surface albedo forcings the cloud fraction always decreases with the positive forcings, so that the shortwave feedback of cloud is positive and the longwave counterpart is negative. The net feedback of cloud is positive to the CO_2 change and negative to the surface albedo change, and the cloud feedback to the solar change is nearly neutral. The difference accounts for the different effects of the forcings on the vertical profile of the atmospheric temperature.

For the hypothetical changes of cloud properties (LWP and effective radius) that may be caused by the indirect effects of aerosols, the cloud feedback sensitivities have to be read differently from the other cases. Sensitivity less than 1 is understood to be a negative feedback effect because the initial forcing is reduced.

TABLE 2. Responses of the model parameters to the external forcings and the changes of cloud properties, and cloud and water vapor feedback sensitivities to the forcings.

	Responses to the forcings			Feedback sensitivities				
Forcing agent	Surface temperature [K (W m^{-2})$^{-1}$]	Lapse rate [K km^{-1} (W m^{-2})$^{-1}$]	Cloud fraction [% (W m^{-2})$^{-1}$]	CWV	Water vapor	Cloud net	Cloud LW	Cloud SW
CO_2 increase	0.91	0.053	−0.68	1.84	1.67	0.168	−0.73	0.9
Solar constant increase	0.6	0.032	−0.33	1.39	1.37	0.0166	−0.07	0.087
Surface albedo decrease	0.89	0.056	−0.8	1.37	1.48	−0.111	−0.23	0.118
Cloud LWP decrease	0.5	0.038	0.9	2.2	1.7	0.502	0.146	0.36
Cloud effective radius increase	0.42	0.032	0.75	1.79	1.34	0.455	0.154	0.3

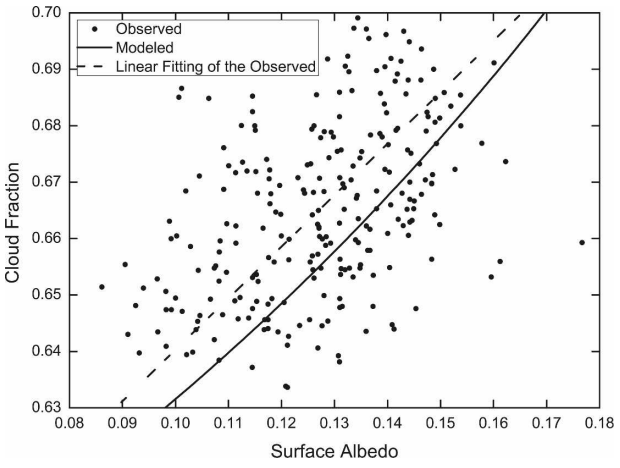

FIG. 3. Responses of the global mean cloud fraction to the global surface albedo. The solid curve is the model result; the dots are the observed monthly data included in the ISCCP D2 dataset and the dashed line is the linear fitting of the data.

For both cases (i.e., a cloud LWP decrease and a cloud effective radii increase), the cloud feedback effects reduce the initial forcing by about a half; however, the total effect of water vapor and cloud is still positive (>1) because of the much stronger positive effect of the water vapor.

The lapse rate in each case increases with the positive forcing and then positively feeds back on the system. The feedback effects have been implicitly included in the longwave feedbacks of the cloud and water vapor, as mentioned above.

As a test of the results, we compare the case for surface albedo forcing to the observed global cloud fraction. In a global mean view, the seasonal variation of global mean temperature is mainly driven by the surface albedo variation, which is partly due to the actual change of surface condition and is partly caused by the sun–earth geometry exposing different parts of the earth surface to the sun during a year. Figure 3 shows the global monthly mean surface albedo (α) and cloud fraction; the correlation is found to be the maximum with a 1-month lag of the cloud fraction data relative to the surface albedo. The linear fitting gives $f = 0.913\alpha + 0.549$, which is compared with the model result (the solid curve) in the figure.

5. Discussion

Because the vertical dimension has been resolved in the model, the convection cannot be simply compared with the EP because it is a function of altitude rather than an integrated value, like EP. Alternatively, the convective flux at a single level contributes to the overall EP locally. The entropy production as defined in Eq. (9) is approximately proportional to the vertical temperature gradient and upward heat flux, and the later is related again to the lapse rate by Eq. (3). Therefore, the local contribution to the total EP at an atmospheric level is approximately proportional to the square of the local convective heat flux so that the MEP in this context is equivalent to the maximum convection. While the equivalence is not a strict validation of the convective hypothesis in Paltridge's models, it implies the possibility of a general application of the MEP principle to climate models with both horizontal and vertical resolutions, without appealing to the additional convective constraint. The magnitude contrast between the EPs resulting from convection ($\sim$40 mW m^{-2} K^{-1} in this work) and advection [$\sim$8.9 mW m^{-2} K^{-1} in Paltridge (1978)] may be the underlying reason why the convective hypothesis has seemed more significant than the MEP principle about the advection heat transport in yielding the climate state close to that observed (O'Brien and Stephens 1995).

Consequently, the EP in the present model is essentially determined by the lapse rate, and the state with MEP is approximately equivalent to the state with the maximum lapse rate, which in principle causes the maximum turbulence. The result that the equilibrium climate system is in a state with the MEP implies that clouds and water vapor are determined at least in the global mean climate state so as to produce the maximum vertical temperature gradient (or lapse rate) as well as the EP. Essentially, the lapse rate is maintained by the heating process (solar heating) at the surface and the cooling process (infrared emission) in the upper troposphere. Both clouds and water vapor have the greenhouse effect warming the surface while cooling the upper troposphere. On the other hand, clouds cool the surface by reflecting the incident solar beam. The model result shows that there is a point for clouds and water vapor to maintain the MEP associated with the vertical turbulence.

On the other hand, the vertical turbulent flux produces entropy by transporting heat from the warmer and lower atmosphere and the surface to the colder and higher atmosphere, while it also tends to mitigate the vertical temperature gradient, which in return reduces the entropy production rate. This situation has been discussed by Kleidon and Lorenz (2005) with a simple box model without a fixed boundary condition, where these two contradictive processes compromise to a unique point with the maximum entropy production rate. It implies that the constraining relation [Eq. (3)] may not be necessary for the model, as suggested by Ozawa and Ohmura (1997). However, this theory does not seem supported by the primary results in this work.

The results provide additional evidence that CWV

can be determined from a macroscopic perspective; that is, in spatiotemporal scales that are large enough to take the system as if it was in a state of dynamic equilibrium and high nonlinearity, CWV is largely determined by its overall radiative and thermodynamic effects on the climate system, and the net effect of the detailed processes in microscopic scale are constrained by the global thermodynamics. Under this constraint, the climate effects of radiative property changes of cloud, which are determined by cloud water path and effective radius, are mitigated by the self-regulation of the cloud fraction. However, the self-regulating behavior of the cloud does not ensure negative feedbacks of cloud to any other external forcings. The above experiments show that the cloud feedback is positive to the changed CO_2, negative to the surface albedo change, and nearly neutral to the solar constant change. While the mechanism considered here (about convection) is different from that in the Paltridge's model (about advection), it is interesting to compare the results of both in regards to the feedback of cloud to CO_2 change, which is nearly neutral globally but varies meridionally in that model (Paltridge et al. 2007). This result is in agreement with an intuition that the MEP of advection may be related to the horizontal distribution of cloud fraction and that of convection to the overall cloud fraction, and the two aspects have to be considered in a complementary way to get a complete picture about the cloud feedback issue. After all, although the results should be better to be taken as qualitative rather than quantitative ones (the values and even the signs may be altered in further refined models), they interestingly reveal the likely different responses of the system, including the cloud and water vapor, the lapse rate, and the surface temperature, to the external forcings, which impact on different components and interact with different physical processes of the climate system.

The experimental results show that the water vapor effects are dominant over those of the cloud, because the water vapor amount in the atmosphere seems more sensitive to the temperature than to the cloudiness. This is largely determined by the highly simplified relation that is assumed [Eq. (5)], which may be qualitatively appropriate to the global mean condition but has to be revised to take more physics into account for the model to work on regional scales. The model shows its potential of adapting to the further revision, because the sensitivity examination about the assumptions shows the model is robust for a wide spectrum of the parameters (k_c, γ_c) and (C_1, C_2), which are the key parameters for convective heat exchange and cloud water vapor exchange, respectively. The results of the numerical experiment also highlight the significance of water vapor in simulating the realistic climate state, as noted by Noda and Tokioka (1983). They resolved the vertical dimension in a 2D zonal mean model with a consistent (but variable) lapse rate assumed throughout the troposphere, instead of Eq. (3) in the present work. However, the water vapor in their model was assumed as given distributions of absolute humidity or relative humidity, either of which implied the variation of water vapor amount was independent of clouds, in contrast to the relationship employed in Eq. (5). That is a likely reason among others why they failed to obtain a reasonable MEP climate state. Nevertheless, it should be kept in mind that the relationship between cloud and water vapor assumed here has to be revised when applied to more general situations with various time or space scales. Moreover, to simulate inhomogeneous distribution of clouds and water vapor over different spatial scales, the model has to consider heat exchange at its lateral boundary and be parameterized to work for much wider ranges of key parameters like solar incidence and surface albedo.

It is always hard to check the effects of climate feedbacks on observations, not only because of the lack of the data but also because it is very difficult to separate the feedbacks from the forcings and to distinguish the feedbacks from each other. The primary validation approach in this work assumes that the seasonal variation of the climate is mainly forced by the surface reflectance, not only by its actual change but also by the earth–sun geometrical variation. This approach naturally separates the important feedback, that is, the surface albedo feedback here taken as a forcing, from the CWV feedbacks. The result is encouraging and can be taken as a good sign for the application of MEP principle to further climate feedback studies.

6. Conclusions

This work investigates the applicability of the MEP principle to the vertical one-dimensional energy balance model. The cloud and water vapor in this model is constrained with the MEP criterion instead of other parameterizations for the so-called subgrid processes. The results show that the global mean cloud fraction is reasonably evaluated with the MEP principle and the model is considerably robust to the assumptions. The tentative simulations of feedbacks of clouds and water vapor show different responses of the climate to the forcings resulting from CO_2, solar incidence, and surface albedo, as well as the responses to the changes in cloud optical properties. The reasonable agreement of the model response to global surface reflectance with the observed global seasonal cloud variation suggests

the MEP principle's potential applicability in studying cloud and water vapor feedbacks from the macroscopic thermodynamic perspective.

Acknowledgments. This study has been funded by the 973 Program of China with Grant Number 2006CB403706 and by the Project 40575051 supported by NSFC. We appreciate the anonymous reviewer's advice on improving the manuscript and leading to some deeper discussions, and we appreciate the inspiring comments from Garth Paltridge during the revision.

REFERENCES

Dewar, R., 2003: Information theory explanation of the fluctuation theorem, maximum entropy production and self-organized criticality in non-equilibrium stationary states. *J. Phys. A Math. Gen.,* **36,** 631–641.

Goody, R., 2007: Maximum entropy production in climate theory. *J. Atmos. Sci.,* **64,** 2735–2739.

Grassl, H., 1981: The climate at maximum entropy production by meridional atmospheric and oceanic heat fluxes. *Quart. J. Roy. Meteor. Soc.,* **107,** 153–166.

Houghton, J. T., Y. Ding, D. J. Griggs, M. Noguer, P. J. van der Linden, and D. Xiaosu, Eds., 2001: *Climate Change: The Scientific Basis*. Cambridge University Press, 881 pp.

Hu, Y. X., and K. Stamnes, 1993: An accurate parameterization of the radiative properties of water clouds suitable for use in climate models. *J. Climate,* **6,** 728–742.

Jentsch, V., 1987: Cloud-ice-vapor feedback in a global climate model. *Irreversible Phenomena and Dynamical Systems Analysis in Geosciences,* C. Nicolis and G. Nicolis, Eds., D. Reidel Publishing, 417–437.

Kiehl, J. T., and K. E. Trenberth, 1997: Earth's annual global mean energy budget. *Bull. Amer. Meteor. Soc.,* **78,** 197–208.

Kleidon, A., and R. Lorenz, 2005: Entropy production by earth system processes. *Non-Equilibrium Thermodynamics and the Production of Entropy: Life, Earth, and Beyond,* A. Kleidon and R. D. Lorenz, Eds., Springer, 1–20.

——, K. Fraedrich, T. Kunz, and F. Lunkeit, 2003: The atmospheric circulation and states of maximum entropy production. *Geophys. Res. Lett.,* **30,** 2223, doi:10.1029/2003GL018363.

Lorenz, R. D., 2003: Full steam ahead—Probably. *Science,* **299,** 837–838.

Manabe, S., and R. T. Wetherald, 1967: Thermal equilibrium of the atmosphere with a given distribution of relative humidity. *J. Atmos. Sci.,* **24,** 241–259.

McClatchey, R. A., R. W. Fenn, J. E. A. Selby, F. E. Volz, and J. S. Garing, 1972: Optical properties of the atmosphere. Air Force Cambridge Research Laboratory Rep. AFCRL-72-0497, 108 pp.

Mitchell, J. F. B., and W. J. Ingram, 1992: Carbon dioxide and climate: Mechanisms of changes in cloud. *J. Climate,* **5,** 5–21.

Mobbs, S. D., 1982: Extremal principles for global climate models. *Quart. J. Roy. Meteor. Soc.,* **108,** 535–550.

Nicolis, G., and C. Nicolis, 1980: On the entropy balance of the Earth-atmosphere system. *Quart. J. Roy. Meteor. Soc.,* **106,** 691–706.

Noda, A., and T. Tokioka, 1983: Climates at minima of the entropy exchange rate. *J. Meteor. Soc. Japan,* **61,** 894–908.

O'Brien, D. M., and G. L. Stephens, 1995: Entropy and climate. II. Simple models. *Quart. J. Roy. Meteor. Soc.,* **121,** 1773–1796.

Ozawa, H., and A. Ohmura, 1997: Thermodynamics of a global-mean state of the atmosphere—A state of maximum entropy increase. *J. Climate,* **10,** 441–445.

——, S. Shimokawa, and H. Sakuma, 2001: Thermodynamics of fluid turbulence: A unified approach to the maximum transport properties. *Phys. Rev. E Stat. Nonlinear Soft Matter Phys.,* **64,** doi:10.1103/PhysRevE.64.026303.

——, A. Ohmura, R. D. Lorenz, and T. Pujol, 2003: The second law of thermodynamics and the global climate system: A review of the maximum entropy production principle. *Rev. Geophys.,* **41,** 1018, doi:10.1029/2002RG000113.

Paltridge, G. W., 1975: Global dynamics and climate—A system of minimum entropy exchange. *Quart. J. Roy. Meteor. Soc.,* **101,** 475–484.

——, 1978: The steady-state format of global climate. *Quart. J. Roy. Meteor. Soc.,* **104,** 927–945.

——, 2001: A physical basis for a maximum of thermodynamic dissipation of the climate system. *Quart. J. Roy. Meteor. Soc.,* **127,** 305–313.

——, G. D. Farquhar, and M. Cuntz, 2007: Maximum entropy production, cloud feedback, and climate change. *Geophys. Res. Lett.,* **34,** L14708, doi:10.1029/2007GL029925.

Pujol, T., 2003: Eddy heat diffusivity at maximum dissipation in a radiative-convective one-dimensional climate model. *J. Meteor. Soc. Japan,* **81,** 305–315.

——, and J. E. Llebot, 1999a: Second differential of the entropy as a criterion for the stability in low-dimensional climate models. *Quart. J. Roy. Meteor. Soc.,* **125,** 91–106.

——, and ——, 1999b: Extremal principle of entropy production in the climate system. *Quart. J. Roy. Meteor. Soc.,* **125,** 79–90.

——, and ——, 2000a: Extremal climatic states simulated by a 2-dimensional model Part I: Sensitivity of the model and present state. *Tellus,* **52A,** 422–439.

——, and ——, 2000b: Extremal climatic states simulated by a 2-dimensional model Part II: Different climatic scenarios. *Tellus,* **52A,** 440–454.

——, and J. Fort, 2002: States of maximum entropy production in a one-dimensional vertical model with convective adjustment. *Tellus,* **54A,** 363–369.

Rossow, W. B., and R. A. Schiffer, 1999: Advances in understanding clouds from ISCCP. *Bull. Amer. Meteor. Soc.,* **80,** 2261–2287.

Shutts, G. J., 1981: Maximum entropy production states in quasi-geostrophic dynamical models. *Quart. J. Roy. Meteor. Soc.,* **107,** 503–520.

Sohn, B. J., and E. A. Smith, 1993: Energy transports by ocean and atmosphere based on an entropy extremum principle. I. Zonal averaged transports. *J. Climate,* **6,** 886–899.

——, and ——, 1994: Energy transports by ocean and atmosphere based on an entropy extremum principle. II. Two-dimensional transports. *Meteor. Atmos. Phys.,* **53,** 61–75.

Toon, O. B., C. P. McKay, T. P. Ackerman, and K. Santhanam, 1989: Rapid calculation of radiative heating rates and photodissociation rates in inhomogeneous multiple scattering atmospheres. *J. Geophys. Res.,* **94,** 16 287–16 301.

Walcek, C. J., 1994: Cloud cover and its relationship to relative humidity during a springtime midlatitude cyclone. *Mon. Wea. Rev.,* **122,** 1021–1035.

Wang, B., H. Liu, and G. Shi, 2000: Radiation and cloud schemes. *IAP Global Ocean-Atmosphere-Land System Model,* X. Zhang et al., Eds., Science Press, 28–49.